Applied Mathematics and Computation
Volume 353, 15 July 2019, Pages 189-207

https://doi.org/10.1016/j.amc.2019.01.046

Modeling, simulation and optimization of a pressure retarded osmosis power station

F. Di Michele
University of L'Aquila, L'Aquila, Italy,
E. Felaco, I. Gasser, A. Serbinovskiy
University of Hamburg, Hamburg, Germany
H. Struchtrup
University of Victoria, Victoria, BC, Canada

January 2, 2019

Abstract

Pressure retarded osmosis (PRO) power plants generate power from mixing of saltwater and freshwater by means of membrane systems. In this paper we present a model which describes the complete power station, suitable to optimize the power station both with respect to system parameters and in operating conditions. Special attention is dedicated to the flow model of the "core" membrane unit. It considers the relevant water and salt flows in the system. It also accounts for irreversible losses in the flow across the membrane as well as through the membrane unit, and in the surrounding pump-turbine system. The model represents a compromise between needed complexity (including the most relevant chemo-physics) and simplicity to allow rapid simulations which is an important prerequisit for optimisation. Finally, we optimise numerically, i.e., the net power output (per membrane area) with respect to geometric parameters, membrane parameters as well as operational parameters such as the applied pressure settings during operation.

1 Introduction

Earth' largest 921 rivers discharge about $37288\,\mathrm{km}^3/\mathrm{y}$ or $1.18 \times 10^9\,\mathrm{litres}/\mathrm{s}$ of freshwater into the worlds oceans [8]. As the freshwater enters the oceans, it mixes with saltwater in an uncontrolled irreversible process and entropy is generated. Whenever an irreversible process occurs, there is an associated potential to produce work.
Thermodynamic analysis reveals that each liter of freshwater flowing into the oceans has a work potential of about $2.75\,\mathrm{kJ}$ that could be extracted by fully controlled mixing. Accordingly, the 921 largest rivers offer a total work potential of $3.245\,\mathrm{TWh}$, which is about one-fifth of the worldwide energy consumption [2]. Of course, not all freshwater discharge will be accessible, and realistic power extraction processes will not be able to deliver the theoretical maximum work per liter, but nevertheless the numbers show that power extraction from reversible mixing

can be a factor in the future energy production [13, 14].
Power production by reversible mixing is based on osmotic processes with suitable membranes. When freshwater and saltwater are brought into contact through a semipermeable membrane that lets only water pass, osmotic forces draw freshwater to the saltwater side, as long as the pressure difference across the membrane is below the osmotic pressure of the saltwater. The strong desire of salt to draw more water is due to the system's propensity to minimize its free energy by increasing the entropy of mixing. Thermodynamically speaking, the difference in chemical potential across the membrane drives the flow of water and offers the opportunity to produce work [17].

The Norwegian company Statkraft (www.statkraft.com) has build a demonstration power plant based on the concept of pressure retarded osmosis (PRO). A sketch of the prototype is shown in Fig. 1, see [3] and [9] or [25] for more details.

Pressure retarded osmosis power plants generally consist of membrane modules, turbine for power generation and pressure exchanger. Fig. 2 shows the graphic representation of the substitute model we use to describe the PRO system design in Fig. 1 and to which we will refer from now on. The pressure exchanger is simply substituted by two parts, a pump and a turbine. The saltwater outflow is not split into two parts (as in the realisation in Fig. 1), turbine and pressure exchanger, but the turbine and the pressure exchanger turbine substitute are put together in a single turbine. This makes no difference in our power balance considerations.

The freshwater and saltwater sides of the membrane unit are usually called feed and draw sides, so we will adjust our notation accordingly. The mass flow J_d^0 of incoming saltwater (draw) enters the system at environmental pressure P_E. Then, the pump compresses it to the pressure P_d^0. The mass flow of incoming freshwater (feed) J_f^0 is pressurized to P_f^0. Both streams then run along a membrane unit.

Inside the membrane unit, freshwater at pressure P_f is brought into contact with saltwater at pressure P_d through the semipermeable membrane. As long as the saltwater pressure is below the osmotic pressure, freshwater will pass through the membrane and mix with saltwater. Because saltwater and freshwater have flow resistance, there are some pressure losses along the membrane unit. The increased mass flow J_d^L of a diluted saltwater with outlet pressure P_d^L drives the turbine and generates electricity. The resulting brackish (saltwater with the lower concentration than seawater) is then discharged back in the environment.

If the freshwater inflow J_f is sufficiently large and the pressure losses are sufficiently small, the power generated by the turbine W_T is greater than the sum of W_P^d and W_P^f, that are the powers needed to pump and to pressurize water in the draw and the feed side. Then, the resulting net power $W_{net} = W_T - W_P^d - W_P^f$ is positive. The power plant design, membrane properties and operating conditions define the pressure losses and the amount of saltwater mass flow, which then – for favorable operating conditions – give a certain net power output. The membrane setup is presented in Fig. 3.

The main flow direction is along the membrane length (x-axis). The channel height is denoted as H, the membrane length and width as L and Z, respectively. In the real application $H \ll L$ and $H \ll Z$, therefore inflow and outflow boundary effects are neglected. Moreover, the temperature is assumed to be a constant for all mass flows. The operating pressures have to be chosen such that the hydraulic pressure difference ΔP is less than the osmotic pressure difference $\Delta\pi$ (see Fig. 7), therefore freshwater is passing through the membranes. The inflow rate of pressurized saltwater J_d^0 increases to the outlet value J_d^L.

As in any thermodynamic system, the amount of power produced will be reduced by irreversible losses such as pressure losses in the pipes, the turbine and the pressure exchanger, friction in the flow through the membrane, and friction inside the membrane unit. The losses depend on the details of construction, e.g., membrane material and thickness, length of flow channels, etc. For a given unit with specified materials and dimensions, system performance depends on the detailed flow setting, in particular the chosen pressures. Also, to have a better model description, it is essential to include relevant effects like salt leakage through the membrane and the negative concentration polarization effect.

The idea to produce energy via osmosis can be traced back to Pattle [19] (1954), and models for PRO have been developed since the 1970's [11, 12, 13, 20]. A thorough historical review is provided by Achilli and Childress [3] (2010). We also refer to the review of Logan and Elimelech [15] (2012).

The near future relevance of this power source is related to technical feasibility and to economic profitability. The main problem for the development of reliable and cost-effective PRO systems appears to be that of providing membranes with the proper behavior and longevity. A crucial value with this respect is the power generation per membrane area. In Achilli and Childress [3] the order of $3.5\,W/m^2$ for seawater is reported. It seems that the value of $5\,W/m^2$ is an important threshold value for future realisations.

In the last few years, the growing relevance of renewable energies and improvements in membrane technology, have sparked new interest on the topic. In particular the modeling and simulation of such power plants has attracted particular interest. Models of different complexity have been proposed, including many of the (known) relevant physical and chemical effects. Important effects in real settings are the reverse salt flow (RSF), the internal and the external concentration polarisation (ICP and ECP). Also, due to the known changes of the various flows, concentrations and pressures along the membrane in flow direction models which resolve the spatial (x) dependence are necessary. Another important issue are realistic boundary conditions for such a power plant. In many theoretical studies inflow conditions are used whereas boundary conditions on the pressures would be more realistic and are much easier to realize. Various studies assume the applied pressure over the membrane to be a given constant quantity and not to be the result of underlying (coupled) flow equations. Finally let us mention that in many studies not the whole power station with the relevant components and losses is considered but only the isolated membrane part.

In Straub et al. [21] a x dependence in the flow equations is introduced, the effects of internal and external concentration polarization and reverse salt flux are taken into account. The pressure difference is used as a input value. Maison et al. [16] introduce the nonlinear coupling of the pressure and pressure differences and the flow direction is resolved in a discrete model. In [18] an energy efficiency analysis is presented. Sung et al. [22] and Sundaramoorthy et al [23] use a 2 dimensional model for the membrane only, the pressure is nonlinearly coupled. In Wang et al. [26] the flow equations are resolved along the flow direction, the pressure difference are introduced in an averaged way.
There are other complex applications where PRO is used as an additional energy recovery system e.g. for reverse osmosis [24].

For a deeper and profound understanding of the possibilities and limitations of PRO systems, accurate models have to be developed and used. In this paper we present a flow model which takes care of all the above described effect and phenomena. It is designed to describe a complete

PRO power plant, with emphasis on the losses in the membrane flow assembly. The system will be characterized by resistance parameters for the flow through the membrane unit (flow parallel to membrane), and through the membrane itself (flow perpendicular to membrane). Parameters of the systems are the flow length L of the membrane unit, some defining properties of the membrane and the various flow pressures.
This leads to a continuous stationary model for both the mass fluxes and the pressures along the membrane in the fresh and the salt water part. As has meanwhile become standard, we include RSF, ICP and ECP [10]. Static mixing of the saltwater with the incoming freshwater is employed to avoid, or at least reduce, concentration polarization, and the resulting flow resistance plays a role for the overall performance of the system. With this the important pressure differences depend on the position along the membrane and are self-consistently and nonlinearly coupled to the local fluxes and densities. We describe the complete power plant by including the pressure exchanger and the power turbines. This leads to a parameter dependent nonlinear Ordinary Differential Equations (ODE) system for which a corresponding boundary value problem has to be solved. To our knowledge presently this model with the described properties is one of the most complete models used to describe a PRO power station. This model allows for fast simulations and thus for optimization approaches, so we can optimize with respect to the various applied pressures and with respect to system parameters. Therefore this model can be applied both in the planning phase and in the operational phase of a PRO power station.

In Section 2 we set up and analyze a one-dimensional mathematical model, that represents the dynamics in the membrane unit. It consists of a simple system of conservation laws for mass and momentum. We complete the model first with one sided boundary value conditions (Section 2.1), as a simplest first case; then a more realistic set-up is considered, assigning the values of the pressures on the boundaries. In Section 2.2 we include the pressurizing pumps and the turbine. In order to evaluate the performance of a complete PRO system we introduce the gross and net power output of the PRO power station and the specific energy (per total volume flow). In Section 3 we scale the system, perform numerical tests and optimize the net power output with respect to system and operating parameters. In Table 6 we collected a list of symbols.

2 Mathematical model

Here we introduce the system of balance laws that we intend to use to model the phenomena described in the previous section. The direction of the membrane width Z has no influence on the system performance, so we normalize any variable $F(x)$ as $\hat{F}(x) = F(x)/Z$. The extended

model for full-scale PRO system is given by

$$\begin{aligned}
\frac{d\hat{J}_{sd}(x)}{dx} &= -J_{s,in}(x),\\
\frac{d\hat{J}_{wd}(x)}{dx} &= J_{w,in}(x),\\
\frac{d\hat{J}_{sf}(x)}{dx} &= J_{s,in}(x),\\
\frac{d\hat{J}_{wf}(x)}{dx} &= -J_{w,in}(x),\\
\frac{dP_d(x)}{dx} &= -\frac{f_{mix}(Re_H)}{4}\frac{\hat{J}_d(x)^2}{\rho_d(x)H^3} - \frac{1}{H^2}\frac{d}{dx}\left[\frac{\hat{J}_d(x)^2}{\rho_d(x)}\right],\\
\frac{dP_f(x)}{dx} &= -\frac{f_{mix}(\bar{R}e_H)}{4}\frac{\hat{J}_f(x)^2}{\rho_f(x)H^3} - \frac{1}{H^2}\frac{d}{dx}\left[\frac{\hat{J}_f(x)^2}{\rho_f(x)}\right].
\end{aligned} \tag{2.1}$$

where the indices *f* and *d* refer to fresh (feed) and salt water (draw) part, respectively. The indices *s* and *w* refer to salt and water, respectively.
The unknowns are six, namely: the salt and water mass flows $\hat{J}_{sf}$, $\hat{J}_{wf}$ and the pressure P_f in the freshwater (feed) part and the corresponding quantities $\hat{J}_{sd}$, $\hat{J}_{wd}$, P_d in the saltwater (draw) part.
The first four equations in (2.1) define at every point x the changes of the mass flows $\hat{J}_f(x)$ and $\hat{J}_d(x)$ due to the water flow per length through the membrane $J_{w,in}$ from the freshwater to the saltwater part and due to the salt flow $J_{s,in}$ from the saltwater to the freshwater part.
The last two equations in (2.1) are the stationary momentum balance in the draw and feed part. Pressure loss is given by friction (first term on the right hand side) and by convection (second term on the right hand side). In the friction term we have the (dimensionless) friction coefficient f_{mix} which depends on the Reynolds number Re_H of the flow.

In the following we will close the system be expressing the remaining quantities - the total mass flows $\hat{J}_f, \hat{J}_d$, the mass densities ρ_f, ρ_d, the water and salt flows $J_{s,in}, J_{w,in}$ through the membrane - as functions of the six unknwons.
We start with the total mass flows in the freshwater and in the saltwater part: these are given by

$$\hat{J}_f(x) = \hat{J}_{sf}(x) + \hat{J}_{wf}(x), \qquad \hat{J}_d(x) = \hat{J}_{sd}(x) + \hat{J}_{wd}(x),$$

respectively.

Next we consider the mass densities in (2.1): the local mass densities of freshwater ρ_f and of saltwater ρ_d are defined as ratios of the corresponding mass and volume flows. Under the assumption of ideal mixing the volume flows $\dot{V}_f$ and $\dot{V}_d$ of the mixture is the sum of volume flows of the unmixed components:

$$\dot{V}_f = \frac{J_{wf}}{\rho_w} + \frac{J_{sf}}{\rho_s}, \qquad \dot{V}_d = \frac{J_{wd}}{\rho_w} + \frac{J_{sd}}{\rho_s} \tag{2.2}$$

where ρ_w and ρ_s are the mass densities of water and salt respectively.
Then local mass density of saltwater can be calculated as the ratio of the local total mass and

volume flows,

$$\rho_d = \frac{J_d}{\dot{V}_d} = \frac{J_{wd} + J_{sd}}{\frac{J_{wd}}{\rho_w} + \frac{J_{sd}}{\rho_s}}. \tag{2.3}$$

Likewise, the local mass density of the freshwater is calculated as

$$\rho_f = \frac{J_f}{\dot{V}_f} = \frac{J_{wf} + J_{sf}}{\frac{J_{wf}}{\rho_w} + \frac{J_{sf}}{\rho_s}}. \tag{2.4}$$

Before we pass to the flows trough the membrane, let us make a comment on the channel height H which plays an important role. The quantity on the left (change of the pressure) is a quantity per unit area (in $Nm^{-2} = kgs^{-2}m$), where the area is intended orthogonal to the x flow direction. Therefore on the right hand side we have mass fluxes per unit area

$$\hat{J}_d/H = J_d/(ZH), \qquad \hat{J}_f/H = J_f/(ZH)$$

(in $kgs^{-1}m^{-2}$) obtained as total mass fluxes J_f, J_d (in kgs^{-1}) divided by the area orthogonal to the flow direction formed by a rectangle of height H and depth Z.
Thus the friction term can be written as

$$-\frac{f_{mix}(Re_H)}{4}\frac{\hat{J}_d(x)^2}{\rho_d(x)H^3} = -\frac{f_{mix}(Re_H)}{2}\frac{1}{2H}\frac{(\hat{J}_d(x)/H)^2}{\rho_d(x)}$$

where the $2H$ in the denominator represents the limit of the so called hydraulic diameter $2HZ/(H+Z)$ for the mentioned $H \times Z$ rectangle for $Z \to \infty$ or $H/Z \to 0$.

To describe the water and salt flows $J_{w,in}$ and $J_{s,in}$ trough the membrane in (2.1) we need (chemo-physical) models. The amount of permeating salt at a fixed point x along the membrane can be modeled by the first Fick's Law [7]. Thus for the mass flow of salt we have

$$J_{s,in} = B\Delta c_{salt}, \tag{2.5}$$

where B is the salt permeability coefficient and Δc_{salt} is the salt concentration difference across the membrane at a fixed point x. The salt concentration difference is given by the difference of the (relative) concentrations

$$\Delta c_{salt}(x) = \frac{\hat{J}_{sd}(x)}{\hat{J}_{sd}(x) + \hat{J}_{wd}(x)} - \frac{\hat{J}_{sf}(x)}{\hat{J}_{sf}(x) + \hat{J}_{wf}(x)}.$$

The mass flow of freshwater through the membrane at a fixed point x along the membrane can be modelled as proportional to the difference of the two competing effects, the pressure difference $\Delta P(x) = P_d(x) - P_f(x)$ and the osmotic pressure difference $\Delta\pi(x) = \pi_d(x) - \pi_f(x)$, where π_d is the osmotic pressure in the draw side and π_f the osmotic pressure in the feed side:

$$J_{w,in} = A\left(\Delta\pi - \Delta P\right). \tag{2.6}$$

A denotes the membrane water permeability coefficient.
At this point the only quantities to define are the osmotic pressures π_F and π_d. To do so we assume that the saltwater is an ideal mixture of water and salt; the osmotic pressure reads [17]

$$\pi = -\rho_w R_w T_0 \ln\left(X_w\right), \tag{2.7}$$

where T_0 is the systems absolute temperature, R_w is the gas constant of water, ρ_w is the mass density of water and X_w is the mole fraction of water in the saltwater.
Assuming the same velocities for water and salt, the mole fraction of water in saltwater is given by

$$X_w = \frac{\frac{\hat{J}_{wd}}{M_W}}{\frac{\hat{J}_{wd}}{M_W} + 2\frac{\hat{J}_{sd}}{M_S}} = \left(1 + \frac{2M_W}{M_S}\frac{\hat{J}_{sd}}{\hat{J}_{wd}}\right)^{-1} \tag{2.8}$$

where M_W is the molecular weight of water and M_S is the molecular weight of salt. The factor 2 accounts for the dissociation of salt crystals into Na^+ and Cl^- ions. Substituting (2.8) into the equation (2.7) gives us the final form of the osmotic pressure.
Therefore the corresponding equations for the draw (saltwater) and feed (freshwater) osmotic pressures are given by

$$\pi_d = \rho_w R_w T_0 \ln\left(1 + \frac{2M_W}{M_S}\frac{\hat{J}_{sd}}{\hat{J}_{wd}}\right)^{-1}, \tag{2.9}$$

$$\pi_f = \rho_w R_w T_0 \ln\left(1 + \frac{2M_W}{M_S}\frac{J_{sf}}{J_{wf}}\right)^{-1}. \tag{2.10}$$

So we can state a first, simple version of the model, completing equations (2.1) with:

$$\begin{aligned} J_{s,in} &= B\left(\frac{\hat{J}_{sd}(x)}{\hat{J}_{sd}(x) + \hat{J}_{wd}(x)} - \frac{\hat{J}_{sf}(x)}{\hat{J}_{sf}(x) + \hat{J}_{wf}(x)}\right), \\ J_{w,in} &= A\left(\Delta\pi - \Delta P\right) = A\left(\rho_w R_w T_0 \ln\frac{\left(1 + \frac{2M_W}{M_S}\frac{\hat{J}_{sf}}{\hat{J}_{wf}}\right)}{\left(1 + \frac{2M_W}{M_S}\frac{\hat{J}_{sd}}{\hat{J}_{wd}}\right)} - \Delta P\right). \end{aligned} \tag{2.11}$$

However, this form form of the model does not include concentration polarization, which is an essential effect for the process we intend to describe. To take into account this effect, we need to slightly modify (2.5) and (2.6). There are two types of concentration polarization effects: the external concentration polarization (ECP) and the internal concentration polarization (ICP). The concentration polarization mechanism is shown in Fig. 4.

The external concentration polarization effect is due to a thin layer of diluted solution appearing both in draw and feed side of the membrane. Assuming perfectly mixed conditions, ECP can be neglected and the external boundary layers can be ignored [11], i.e. we set the salt concentrations $c_1 = c_2$, $c_4 = c_5$ and the osmotic pressures $\pi_1 = \pi_2$, $\pi_4 = \pi_5$ (see Fig. 4). Thus from now on we can set $\pi_d = \pi_1 = \pi_2$ and $\pi_f = \pi_4 = \pi_5$.
To include the internal concentration polarization we follow [11], where a model for the water mass flow through the membrane is derived:

$$J_{w,in} = A\left[\frac{\pi_d - \pi_f \exp\left(J_{w,in}K\right)}{1 + \frac{B}{J_{w,in}}\left[\exp\left(J_{w,in}K\right) - 1\right]} - \Delta P\right]. \tag{2.12}$$

Here K is the internal concentration polarization mass transfer coefficient of the membrane support layer, namely a measure of the resistance to salt transport in the porous support. It can be represented as $K = S/D_s$, that is the ratio of a structural parameter S and the salt diffusion coefficient of the membrane D_s. The structure parameter is given by $S = \tau t/\epsilon$ where τ is the tortuosity, ϵ is the porosity and t is the thickness of the membrane.

It is easy to see that for no internal concentration polarization (i.e. $K = 0$, $S = 0$, $\tau = 0$) we obtain immediately the simple model (2.11) from above.
Note that te equation (2.12) is not explicit for $J_{w,in}$ but it can be simplified by expanding $\exp(J_{w,in}K)$ for small $J_{w,in}K$. Then, (2.12) transforms into

$$J_{w,in} = A\left[\frac{\pi_d - \pi_f\left(1 + J_{w,in}K\right)}{1 + BK} - \Delta P\right] \tag{2.13}$$

and thus the related explicit form of $J_{w,in}$ is computed solving (2.13):

$$J_{w,in} = -A\frac{\pi_f - \pi_d + \Delta P\left(1 + BK\right)}{1 + K\left(B + A\pi_f\right)}. \tag{2.14}$$

Let us finally discuss the coefficients A and B. The water permeability coefficient A is usually obtained experimentally or given by the membrane manufacturer. However, assuming also an independent given (constant) salt permeability coefficient B is not realistic. B depends in general on the value of A. This is the last refinement of the model we have to discuss. The relation is given by

$$B = B(x) = \frac{A(1 - R)(\Delta\pi - \Delta P)}{R}, \tag{2.15}$$

where R is the salt rejection coefficient (amount of rejected salt in %), which is usually given by the membrane manufacturer. As B now depends on $\Delta\pi$ and ΔP, it becomes also space dependent. Equation (2.15) shows that the high water permeability trades-off with the low salt selectivity and, vice versa, high salt selectivity of the membrane results in low water permeability.
So we can finally write an updated version of (2.11) that includes internal concentration polarization effects:

$$\begin{aligned} J_{w,in}(x) &= -A\frac{\pi_f(x) - \pi_d(x) + \Delta P(x)\left(1 + B(x)K\right)}{1 + K\left(B(x) + A\pi_f(x)\right)}, \\ J_{s,in}(x) &= B(x)\Delta c_{salt}(x), \\ B(x) &= \frac{A(1 - R)(\Delta\pi(x) - \Delta P(x))}{R}. \end{aligned} \tag{2.16}$$

The complete set of equations (2.1) together with the definitions of the various terms in this section have to be completed with additional boundary conditions.

2.1 Boundary conditions

The differential equations (2.1) have to be equipped with boundary conditions. One possibility is to prescribe conditions for the six unknowns at the right boundary (entrance), i.e.

:

$$
\begin{aligned}
\hat{J}_{sd}(x)|_{x=0} &= \hat{J}^0_{sd} = \frac{\hat{J}^0_{sd}}{\hat{J}^0_d}\hat{J}^0_d \\
\hat{J}_{wd}(x)|_{x=0} &= \hat{J}^0_{wd} = \frac{\hat{J}^0_{wd}}{\hat{J}^0_d}\hat{J}^0_d \\
\hat{J}_{sf}(x)|_{x=0} &= \hat{J}^0_{sf} = 0, \\
\hat{J}_{wf}(x)|_{x=0} &= \hat{J}^0_{wf} = \hat{J}^0_f, \\
P_s(x)|_{x=0} &= P^0_s, \\
P_f(x)|_{x=0} &= P^0_f.
\end{aligned}
\tag{2.17}
$$

Mathematically the problem with this conditions becomes an initial value problem (IVP). The coefficients $\hat{J}^0_{sd}/\hat{J}^0_d$ and $\hat{J}^0_{wd}/\hat{J}^0_d$ are the salt and the water mass fractions in the incoming saltwater assuming a salinity of $\hat{J}^0_{sd}/\hat{J}^0_{wd}$. There is no incoming salt in the freshwater part ($\hat{J}^0_{sf} = 0$), and the total incoming saltwater flow $\hat{J}^0_d$ and total incoming freshwater flow $\hat{J}^0_f$ will be assumed to be equal (see example in Table 4). To our knowledge this type of boundary conditions was used in all models from the literature where a detailed x dependence of the quantities (along the flow in the membrane) is described (e.g. [16, 21, 26]).

However, in reality controlling saltwater J^0_d and freshwater J^0_f inflow rates is difficult, mainly because of high dependency on the membrane unit design. Clearly, membrane module geometry is fixed and cannot change once it is manufactured. Technically the control of the fluxes would be realized by using the pumps at the entrances and therefore choosing appropriate pressures P^0_f and P^0_d. Therefore it is natural to prescribe directly the pressures on the two sides. Thus, we would like to determine the incoming draw and feed flow rates with respect to chosen in and out-let saltwater and freshwater pressures. To answer this question, we have to formulate a two sided boundary value problem.
We need to equip the model with 6 conditions. First, we start with saltwater P^0_d and freshwater P^0_f inlet pressures. Also we prescribe saltwater and freshwater outlet pressures P^L_d and P^L_f respectively. Then, we assume that incoming feed flow consists of pure water only, $J^0_{sf} = 0$.
To find the last missing condition we will introduce a new function, the mass fraction on the draw side $C_d(x)$, a quantity that we can compute easily and that we can prescribe at $x = 0$.
The salt to water mass fraction in the draw side of the membrane is given as the ratio of salt to pure water flow:

$$
C_d(x) = \frac{\hat{J}_{sd}(x)}{\hat{J}_{wd}(x)} \quad \text{or} \quad \hat{J}_{sd}(x) = C_d(x)\hat{J}_{wd}(x). \tag{2.18}
$$

Differentiating $\hat{J}_{sd}(x)$ with respect to x and combining with the first equation from (2.1) gives

$$
\frac{d\hat{J}_{sd}(x)}{dx} = \frac{dC_d(x)}{dx}\hat{J}_{wd}(x) + \frac{d\hat{J}_{wd}(x)}{dx}C_d(x) = -J_{s,in}(x). \tag{2.19}
$$

Then, we can write the differential equation for salt to water mass fraction in the draw side as

$$
\frac{dC_d(x)}{dx} = -\frac{J_{s,in}(x) + \dfrac{d\hat{J}_{wd}(x)}{dx}C_d(x)}{\hat{J}_{wd}(x)}. \tag{2.20}
$$

Changing the first equation in (2.1) to (2.20) will result in the following model:

$$\begin{aligned}
\frac{dC_d(x)}{dx} &= -\frac{J_{s,in}(x) + \frac{d\hat{J}_{wd}(x)}{dx}C_d(x)}{\hat{J}_{wd}(x)},\\
\frac{d\hat{J}_{wd}(x)}{dx} &= J_{w,in}(x),\\
\frac{d\hat{J}_{sf}(x)}{dx} &= J_{s,in}(x),\\
\frac{d\hat{J}_{wf}(x)}{dx} &= -J_{w,in}(x),\\
\frac{dP_d(x)}{dx} &= -\frac{f_{mix}(Re_H)}{4}\frac{\hat{J}_d(x)^2}{\rho_d(x)H^3} - \frac{1}{H^2}\frac{d}{dx}\left[\frac{\hat{J}_d(x)^2}{\rho_d(x)}\right],\\
\frac{dP_f(x)}{dx} &= -\frac{f_{mix}(\bar{R}e_H)}{4}\frac{\hat{J}_f(x)^2}{\rho_f(x)H^3} - \frac{1}{H^2}\frac{d}{dx}\left[\frac{\hat{J}_f(x)^2}{\rho_f(x)}\right].
\end{aligned} \tag{2.21}$$

In the equations above, updated terms $\rho_d(x)$, $\Delta c_{salt}(x)$, $\hat{J}_d(x)$ and $J_{s,in}(x)$ are given as

$$\begin{aligned}
&\rho_d(x) = \frac{C_d(x)+1}{\frac{1}{\rho_S}C_s(x) + \frac{1}{\rho_W}}, \qquad \Delta c_{salt}(x) = \frac{C_s(x)}{C_s(x)+1} - \frac{\hat{J}_{sf}(x)}{\hat{J}_{sf}(x)+\hat{J}_{wf}(x)},\\
&\hat{J}_d(x) = C_d(x)\hat{J}_{wd}(x) + \hat{J}_{wd}(x), \qquad J_{s,in}(x) = B(x)\Delta c_{salt}(x).
\end{aligned} \tag{2.22}$$

We can finally introduce the boundary conditions for equations (2.21) (see example in Table 5):

$$\begin{aligned}
C_d(x)|_{x=0} &= C_d^0 = \frac{\hat{J}_{sd}^0}{\hat{J}_{wd}^0},\\
\hat{J}_{sf}(x)|_{x=0} &= 0\,kg/s,\\
P_d(x)|_{x=0} &= P_d^0,\\
P_d(x)|_{x=L} &= P_d^L,\\
P_f(x)|_{x=0} &= P_f^0,\\
P_f(x)|_{x=L} &= P_f^L = P_E.
\end{aligned} \tag{2.23}$$

Some of these quantities are fixed: $C_d^0 = \hat{J}_{sd}^0/\hat{J}_{wd}^0$ is the salinity of the incoming saltwater; P_f^L also does not change as the freshwater channel does not end up in a turbine, so we have see level standard external pressure; finally the incoming salt flow in the feed side $\hat{J}_{sf}^0$ is 0.
We are left with three parameters, P_d^0, P_d^L and P_f^0, that we may discuss to obtain the optimal set of the operating pressures.

Since we do not know which type of conditions will prevail in future applications of such models, in this paper we use them both. Although the two sided conditions are numerically more costly, we believe that the two sided pressure conditions are easier to combine with realistic settings in experiments. Therefore we would propose to use the two sided conditions in the future.

2.2 Net Power

To complete the model, we introduce a suitable expression for the net power produced by the PRO power plant:

$$W_{net} = W_T - W_P^d - W_P^f, \tag{2.24}$$

where W_T is turbine power production, W_P^d is pump power demand to pressurize saltwater and W_P^f is pump power demand to pressurize freshwater.
Saltwater pump pressurizes incoming seawater to pressure P_d^0, hence we can define

$$W_P^d = \frac{1}{\epsilon_P}\frac{J_d^0}{\rho_d^0}\left(P_d^0 - P_E\right). \tag{2.25}$$

Here, ρ_0 is the mass density of incoming saltwater, ϵ_P is the pump efficiency, J_d^0/ρ_d^0 is the volume flow of the incoming saltwater and P_E is environmental pressure.
The pump power to pressurize freshwater is given by

$$W_P^f = \frac{1}{\epsilon_P}\frac{J_f^0}{\rho_f^0}\left(P_f^0 - P_E\right). \tag{2.26}$$

The turbine is driven by the pressure difference between P_d^L and P_E. Therefore, we can describe the turbine power generation as

$$W_T = \epsilon_T\frac{J_d^L}{\rho_d^L}\left(P_d^L - P_E\right), \tag{2.27}$$

where ρ_L is the mass density of exiting saltwater, ϵ_T is the turbine efficiency and J_d^L/ρ_d^L is the volume flow of exiting saltwater.
If $\epsilon_P = 1$ then the pump is fully reversible. However, the typical pump efficiencies are around $95\,\%$ and for the turbine $90\,\%$. For sake of simplicity, we will assume $\epsilon_P = \epsilon_T$.
The power per width Z, $\hat{W}_{net}$, is given by

$$\begin{aligned}
&\hat{W}_{net} = \hat{W}_T - \hat{W}_P^d - \hat{W}_P^f \\
&\hat{W}_T = \epsilon_T\frac{\hat{J}_d^L}{\rho_d^L}\Delta P_d^L, \quad \hat{W}_P^d = \frac{1}{\epsilon_P}\frac{\hat{J}_d^0}{\rho_d^0}\Delta P_d^0, \quad \hat{W}_P^f = \frac{1}{\epsilon_P}\frac{\hat{J}_f^0}{\rho_f^0}\left(P_f^0 - P_E\right).
\end{aligned}$$

A more common and useful criteria to estimate PRO system performances is the power per membrane area, defined as:

$$\bar{W}_{net} = \frac{\hat{W}_{net}}{L} = \frac{W_{net}}{ZL}, \tag{2.28}$$

where L is the membrane length.
In Section 4, when evaluating the performances of our model, we will use mainly $\bar{W}_{net}$; however it is worth mentioning another quantity that can be useful to estimate PRO system performance, the specific energy, that is the energy extracted per total volume of the feed and draw solutions combined. In our notation the specific energy is:

$$SE = \frac{W_{net}}{J_d^0/\rho_d^0 + J_f^0/\rho_f^0}, \tag{2.29}$$

measured in kWh/m^3.

3 Numerical Simulations

3.1 Scaling

Before discussing the numerical results, we scale the equations in order to better understand the relevant dimensionless parameters and the role of the various terms. We use the reference values listed in Table 1. The values are of the same order of the ones in [16] and refer to a full scale PRO system. Contrary to that often "coupon-scale" examples are considered for both simulations and experiments (see e.g. [16, 21]).

We remark that for every scaled quantity we set $\tilde{f} = f/f_r$. In order to avoid a too heavy notation we use the same symbols for the scaled quantities (without $\tilde{()}$).
The scaled equations for the one sided IVP are:

$$\begin{aligned}
\frac{d\hat{J}_{sd}(x)}{dx} &= -\gamma J_{s,in}(x),\\
\frac{d\hat{J}_{wd}(x)}{dx} &= \gamma J_{w,in}(x),\\
\frac{d\hat{J}_{sf}(x)}{dx} &= \gamma J_{s,in}(x),\\
\frac{d\hat{J}_{wf}(x)}{dx} &= -\gamma J_{w,in}(x),\\
\frac{dP_d(x)}{dx} &= -\frac{f_{mix}(Re_H)}{4}\frac{\hat{J}_d(x)^2}{\rho_d(x)} - b\frac{d}{dx}\left[\frac{\hat{J}_d(x)^2}{\rho_d(x)}\right],\\
\frac{dP_f(x)}{dx} &= -\frac{f_{mix}(\bar{Re}_H)}{4}\hat{J}_f(x)^2\rho_f(x) - b\frac{d}{dx}\left[\frac{\hat{J}_f(x)^2}{\rho_f(x)}\right],
\end{aligned} \tag{3.1}$$

with parameters

$$\gamma = \frac{x_r^2 A P_r}{J_r C_r} \sim 2.5\cdot 10^{-2} \qquad b = \frac{H}{x_r} \sim 10^{-4}. \tag{3.2}$$

The convection term in the equations for pressure has a smaller effect than the friction term (as long as no rapid changes in x occur).
The amount of permeate salt $J_{s,in}(x)$ and water $J_{w,in}(x)$ as well as the feed $\hat{J}_f(x)$ and draw $\hat{J}_d(x)$ flows are given as

$$\begin{aligned}
\hat{J}_d(x) &= \hat{J}_{sd}(x) + \hat{J}_{wd}(x),\\
\hat{J}_f(x) &= \hat{J}_{sf}(x) + \hat{J}_{wf}(x),\\
J_{w,in}(x) &= -\frac{\pi_f(x) - \pi_d(x) + \Delta P(x)\left(1 + AP_rKB(x)\right)}{1 + AP_rK\left(B(x) + \pi_f(x)\right)},\\
J_{s,in}(x) &= B(x)\Delta c_{salt}(x),
\end{aligned} \tag{3.3}$$

where $\pi_f(x)$ and $\pi_d(d)$ are the osmotic pressures at feed and draw sides of the membrane unit, respectively. Additionally, total local densities, salt concentration difference across the membrane, salt permeability coefficient, salt diffusion coefficient and structural parameter of the membrane support layer, as well as Reynolds number and friction factor are of the following

form:

$$
\begin{aligned}
\rho_d(x) &= \frac{\hat{J}_{sd}(x)+\hat{J}_{wd}(x)}{\frac{\rho_W}{\rho_S}\hat{J}_{sd}(x)+\hat{J}_{wd}(x)}, & \rho_f(x) &= \frac{\hat{J}_{sf}(x)+\hat{J}_{wf}(x)}{\frac{\rho_W}{\rho_S}\hat{J}_{sf}(x)+\hat{J}_{wf}(x)},\\
\Delta c_{salt}(x) &= \frac{\hat{J}_{sd}(x)}{\hat{J}_d(x)}-\frac{\hat{J}_{sf}(x)}{\hat{J}_f(x)}, & \Delta\pi &= \pi_d-\pi_f,\\
\pi_d &= \frac{\rho_w R_w T_0}{P_{ref}}\ln\left(1+\frac{2M_W}{M_S}\frac{\hat{J}sd}{\hat{J}wd}\right)^{-1}, & \pi_f &= \frac{\rho_w R_w T_0}{P_{ref}}\ln\left(1+\frac{2M_W}{M_S}\frac{\hat{J}sf}{\hat{J}wf}\right)^{-1},\\
\Delta P &= P_d-P_f, & B(x) &= \frac{(1-R)(\Delta\pi(x)-\Delta P(x))}{R},\\
Re_H &= \frac{J_r}{x_r}\frac{\hat{J}(x)}{2\eta}, & K &= \frac{S}{D_s},\\
f_{mix} &= \frac{96}{Re_H}\left(4.86+0.65\sqrt{Re_H}\right), & S &= \frac{\tau t}{\epsilon}.
\end{aligned}
\tag{3.4}
$$

The scaled equations for the two sided BVP are:

$$
\begin{aligned}
\frac{dC_d(x)}{dx} &= -\frac{\gamma J_{s,in}(x)+\frac{d\hat{J}_{wd}(x)}{dx}C_d(x)}{\hat{J}_{wd}(x)},\\
\frac{d\hat{J}_{wd}(x)}{dx} &= \gamma J_{w,in}(x),\\
\frac{d\hat{J}_{sf}(x)}{dx} &= \gamma J_{s,in}(x),\\
\frac{d\hat{J}_{wf}(x)}{dx} &= -\gamma J_{w,in}(x),\\
\frac{dP_d(x)}{dx} &= -\frac{f_{mix}(Re_H)}{4}\frac{\hat{J}_d(x)^2}{\rho_d(x)}-b\frac{d}{dx}\left[\frac{\hat{J}_d(x)^2}{\rho_d(x)}\right],\\
\frac{dP_f(x)}{dx} &= -\frac{f_{mix}(Re_H)}{4}\frac{\hat{J}_f(x)^2}{\rho_f(x)}-b\frac{d}{dx}\left[\frac{\hat{J}_f(x)^2}{\rho_f(x)}\right],
\end{aligned}
\tag{3.5}
$$

with B, $\hat{J}_f$, $J_{w,in}$ from (3.3) and

$$
\begin{aligned}
\hat{J}_d(x) &= C_d(x)\hat{J}_{wd}(x)+\hat{J}_{wd}(x),\\
\rho_d(x) &= \frac{C_s(x)+1}{\frac{\rho_w}{\rho_S}C_s(x)+1},\\
\Delta c_{salt}(x) &= \frac{C_d(x)}{C_d(x)+1}-\frac{\hat{J}_{sf}(x)}{\hat{J}_{sf}(x)+\hat{J}_{wf}(x)}.
\end{aligned}
\tag{3.6}
$$

Finally, we remark that also the one sided (2.17) and two sided boundary conditions (2.23), the net power (2.28) and the specific energy (2.29) have to be scaled. The fluxes are scaled by J_r, the pressures by P_r, C_d is already a dimensionless quantity. The net power W_{net} is scaled by the

reference values $\frac{J_r P_r}{\rho_r}$, $\bar{W}_{net}$ accordingly by $\frac{J_r P_r}{\rho_r Z L}$; for the specific energy we use the reference value P_r.

Now we can start with some simulations. We mention that the aim of the paper is to show the qualitative properties of the proposed model. Standard parameter sets from the literature are used in order to verify the qualitative behaviour. The parameters characterizing the membrane are summed up in Table 2, while in Table 3 we introduce the remaining quantities included in our set up. For the membrane parameter we refer to [11] and also to [4, 16, 21] where a similar set of parameters for the PRO related considerations and simulations are used. Note that the salt permeability B is not prescribed as a fixed parameter but given by the relation (3.4).

First we start our simulations by considering those as fixed parameters and secondly we will discuss the dependence on the most relevant ones.

Let us mention that all numerical simulations are done in Matlab using standard initial and boundary value problem solvers. Since the direct simulations are extremely fast and robust, we optimize "by hand" running through the parameter ranges under consideration.

3.2 Prescribed data at the inflow side: Initial value problem

The one sided boundary conditions we start with are listed in Table 4. As already mentioned, it is very common to use such kind of conditions where the fluxes have to be prescribed, although the practical realisation is non trivial. We assume purely sweet water at the fresh water side inlet and apply an overpressure for both the fresh water and the draw water side, to make sure that a flow dynamics is induced.
We start by visualizing the behavior of flux and pressure along x in the saltwater and in the freshwater channels (Fig. 5). The behaviour corresponds to our expectations, the total flow in the draw side is increasing, in the fresh water side decreasing. This is due to the water passing through the membrane (see Fig. 6). For the change of the volume flow the salt flow through the membrane plays a minor role. The pressure losses in both sides can also be seen. Interesting is the relation between the different pressures along the flow direction in Fig. 7. For very simple models the maximal power output is expected for $\Delta P = (\Delta\pi/2)$ (see [4]). In reality this ratio will assume certain values and change along the flow direction, as we can also observe in the simulation in the last panel of Fig. 7. Notice that the operating condition are prescribed so that $\Delta P < \Delta\pi$.
Now we start to look for optimal operating conditions. In Fig. 8 we see how the net power per area $\bar{W}_{net}$ depends on the values assigned to initial pressures (a) and to initial flux (b). We have $\max(\bar{W}_{net}) \sim 1.9\, Watt/m^2$ and we obtain a first set of optimal values for the parameters P_d^0, P_f^0, J_d^0, J_f^0.
We can also look for optimal system parameters when designing a power plant. An interesting parameter is the membrane length L. In Fig. 9 we see its influence on both the net power and the specific energy. The power output becomes optimal at a certain lenght, for longer membranes the losses become again dominant. The optimum with respect the specific energy is reached at a much higher length, at about $7\,m$. This is not surprising, since the optimised target function was different.
Next we compare the influence of the different physical effects. In Fig. 10(a) we compare the power per membrane area obtained with our complete model, without the effects of internal

concentration polarization (i.e., $K = 0$), and with the ideal assumption of a membrane completely impermeable to salt (i.e., $R = 100\%$ and $B = 0$). We conclude that these effects have a non negligible impact on the results, in this example up to $15\,\%$. Therefore it is necessary to include these effects.
In Fig. 10(b) we compare the gross (turbine) power output and the net power output. The former is monotonically increasing in the applied pressure difference (between draw and fresh water input), the latter has the already know optimal (maximum) value.

3.3 Prescribed pressures at in- and outflow.

As already discussed the most realistic data to be described at the boundaries are the applied pressures. However, we only have 4 applied pressures but the structure of the set of equations requires 6 conditions. The 2 missing conditions are obtained almost naturally, the vanishing salt content at the fresh water input and the salt concentration at the salt water input given by $35/983$ as the standard average for sea water. These boundary data are summarized in Table 5.
We assume the freshwater outlet pressure as the standard ambient pressure since there is no pump, turbine or similar. We are left with P_d^0, P_d^L and P_f^0, as parameters that we are able to control, by controlling the two pumps at $x = 0$ and the turbine in $x = L$. The only restriction that we require on these quantities are $P_d^0 > P_d^L$ and $P_f^0 > P_f^L$, in order to keep the flow from right to left.
After investigating the dependence of the net power production on these three pressures, we will look at the main parameters given in Table 2 and Table 3.

In Fig. 11 (a) we see how the power production depends on the pressures that we assign at the inlet and at the end of the saltwater channel. Here we are considering only the case $P_s^0 > P_s^L$, a left to right flow, with P_d^0, $P_d^L \in [1.1, 1.4] \cdot 10^6\ Pa$. We obtain the maximal value for net power of $\max(W_{net}) = 1.8954\, W/m^2$, at $P_d^0 = 1.247 \cdot 10^6\ Pa$ and $P_d^L = 1.2349 \cdot 10^6\ Pa$ (about $12\, bar$ over pressure). A huge part of the energy produced is balanced by that consumed in the pump. And we see that there is a linear relation between the P_d^0 and P_d^L for the highest values (the red area in Fig. 11 (a)) .
In Fig. 11 (b) we explore the dependence on the pressure at the inlet of the fresh water; according to our set-up this is due to the pressurizing pump, here with $P_f^0 \in [1, 1.5] \cdot 10^5\ Pa$, while the left side of the fresh water pipe is free, with constant pressure $P_E = 10^5\ Pa$. Increasing P_f^0 helps increasing the power production, until the costs for the pump weight too much in the net power computation, and W_{net} starts decreasing. With this we have a good idea for which triple of (P_d^0, P_d^L, P_f^0) we obtain the highest net power (per area) production.

Having an idea about the optimal pressure boundary data, we can begin to investigate some of the other relevant parameters of our set up. We vary the geometry and the efficiencies of the pump and the turbine, and investigate both the net power (per area) output and the specific energy.
In Fig. 12 we vary the length of the membrane (along the flow direction) and see an optimal value of about $2\, m$ for the net power output and a higher value (about $5 - 6\, m$) for the specific energy. For short membranes we do not transfer enough fresh water to the salt water side, for long membranes the losses (in pressure due to friction) become dominant.
Similar, the situation for the channel height H in Fig. 13(a). For small H the frictional losses dominate, for large H the transfered freshwater through the membrane (related to the flux in the salt water part) looses importance.

In Fig. 13(b) we study the dependence of the net power on the pump and turbine efficiency ϵ assumed to be equal. The dependence is linear with a strong ratio, i.e. an increase of the efficiency from of $5\,\%$ increases the net power per area by $1\,W/m^2$. For the data set used there is a lower threshold at 85% below which we cannot gain power.
In Fig. 14 we summarize the effects of the parameters characterizing the membrane: the ICP mass transfer coefficient K, the water permeability A and the salt rejection R. As expected, increasing K decreases the power output (seemingly linear). There is a lower threshold for the water permeability A, above the threshold there is a nonlinear direct relation between A and the power output. Also, there is a lower threshold for the salt rejection R, above that value there is (seemingly) linear relation between R and net power output. We see that the proposed model offers the possibility to investigate the dependence of the highly relevant quantities net power output and specific energy on system parameters or on control quantities such as boundary data.

4 Conclusions

We present a model which gives an overall description of a PRO power station with the aim of optimizing key quantities such as net power output or specific energy. The model describes the detailed dependence of the quantities along the flow in the membrane (x dependence), which results to be essential due to the significant changes of the quantities in that direction. This approach makes it possible to include a precise description of the nonlinear coupling of the pressures at each position along the flow in the membrane. We discuss to different possibilties of boundary conditions and propose the two sided boundary conditions for future applications. In addition - as it is meanwhile standard in the membrane literature - we include reverse salt flow and internal and external concentration polarisation along the membrane.

We consider the presented model as a step towards accurate modeling of PRO systems. Our results show that PRO performance can vary drastically with design and settings, and thus underlines the need and usefulness of reliable and robust models for PRO performance optimization. We believe that our model includes the most relevant known chemo-physical effects to be considered for a PRO system. On the other hand the model is simple enough to allow for optimizing with respect to system and operational parameters.
We are convinced that models of this type can significantly contribute in the design and the development of future PRO systems. Exact models like the presented one can be used i.e. to further evaluate advanced configurations with multi-staging [5], or combined reverse and forward osmosis processes for energy storage [6].

References

[1] http://www.yuvaengineers.com/wp-content/uploads/2010/04/osmotic-power-7.jpg

[2] INTERNATIONAL ENERGY AGENCY (2018), *2012 Key World Energy Statistics*, http://www.iea.org/publications/freepublications/, IEA.

[3] ACHILLI A., CHILDRESS A.E. (2010), *Pressure retarded osmosis: From the vision of Sidney Loeb to the first prototype installation* – Review, Desalination 261, pp. 205-211.

[4] ACHILLI A., CATH T. Y., CHILDRESS A. E. (2009), *Power generation with pressure retarded osmosis: an experimental and theoretical investigation*, Desalination, 343, pp. 42-52.

[5] BHARADWAJ D., FYLES T.M., STRUCHTRUP H. (2016), *Multistage Pressure Retarded Osmosis*, J. Non-Equilibrium Thermodynamics, 41, pp. 327-347.

[6] BHARADWAJ D., STRUCHTRUP H. (2017), *Large scale energy storage using multistage osmotic processes: Approaching high efficiency and energy density*, Sustainable Energy & Fuels, 1, pp. 599-614.

[7] CRANK J., (1980), *The Mathematics of Diffusion*, Oxford Science Publications.

[8] DAI A., TRENBERTH K.E. (2012), *Estimates of freshwater discharge from continents: latitudinal and seasonal variations*, Journal of Hydrometeorology 3, pp. 660-687.

[9] GERSTANDT K., PEINEMANN K.V., SKILHAGEN S.E., THORSEN T., HOLT T. (2008), *Membrane processes in energy supply for an osmotic power plant. Desalination*, 224 (1), pp. 64-70.

[10] HE W., WANG Y., SHAHEED M.H. (2014), *Modelling of osmotic energy from natural salt gradients due to pressure retarded osmosis: Effects of detrimental factors and flow schemes*, Journal of Membrane Science, 471, pp. 247-257.

[11] LEE K. L., BAKER R. W., LONSDALE H. K. (1981), *Membranes for power generation by pressure-retarded osmosis*, Journal of Membrane Science, 27, pp. 141-171.

[12] LOEB S. (1976), *Production of electric power by mixing fresh and salt water in hydroelectric pile*, Journal of Membrane Science, 1, pp. 49-63.

[13] LOEB S., NORMAN R. (1975), *Osmotic power plants*, Science, 189, pp. 654-655.

[14] LOEB S., VAN HESSEN F., SHAHAF D., (1976) *Production of energy from concentrated brines by pressure-retarded osmosis, II. experimental results and projected energy costs*, Journal of Membrane Science, 1, pp. 249-269.

[15] LOGAN B. E., ELIMELECH M. (2012), *Membrane-based processes for sustainable power generation using water*, Nature 488, pp. 313-319.

[16] MAISONNEUVE J., PILLAY P., LAFLAMME C.B. (2015), *Pressure-retarded osmotic power system model considering non-ideal effects*, Renewable Energy, 75 (2015), pp. 416-424.

[17] STRUCHTRUP H. (2014), *Thermodynamics and Energy Conversion*, Springer, Heidelberg.

[18] *O'Toole G., Jones L., Coutinho C., Hayes C., Napoles M., Achilli A. (2016), River-to-sea pressure retarded osmosis: Resource utilization in a full-scale facility*, Desalination, 389, pp. 39-51.

[19] PATTLE R. (1954), *Production of electric power by mixing fresh and salt water in hydroelectric pile*, Nature, 174, pp. 660-660.

[20] PATTLE R. (1974), *Water salination: a source of energy*, Science, 186, pp. 350-352.

[21] STRAUB A. P., LIN S., ELIMELECH M. (2014), *Module-Scale Analysis of Pressure Retarded Osmosis: Performance Limitations and Implications for Full-Scale Operation*, Environmental Science & Technology, 48, pp. 12435-12444.

[22] SUNG-SOO HONG, WON RYOO, MYUNG-SUK CHUN, SEUNG OH LEE, GUI-YUNG CHUNG (2014), *Numerical studies on the pressure-retarded osmosis (PRO) system with the spiral wound module fo power generation*, Desalination and Water Treatment, 52, pp. 6333-6341.

[23] SUDARAMOORTHY S., SRINIVASAN G., MURTHY D.V.R. (2011), *An analytical model for spiral wound reverse osmosis membranes modules: Part I- Model development and parameter estimation*, Desalination, 280, pp. 403-411.

[24] SENTHIL S., SENTHILMURUGAN S.(2016), *Reverse osmosis-pressure retarded osmosis hybrid systems: modelling, simulation and optimisation*, Desalination, 389, pp. 78-97.

[25] TORLEIF H., THORSEN, T. ET AL. (2009), *Semi-permeable membrane for use in osmosis, and method and plant for providing elevated pressure by osmosis to create power*, 28 2019. US Patent 7,566,402.

[26] WANG Z., HOU D., LIN S. (2016), *Gross vs. net energy: Towards a rational framework for assessing the practical viability of pressure retarded osmosis*, J. of Membrane Science, 503, pp. 132-147.

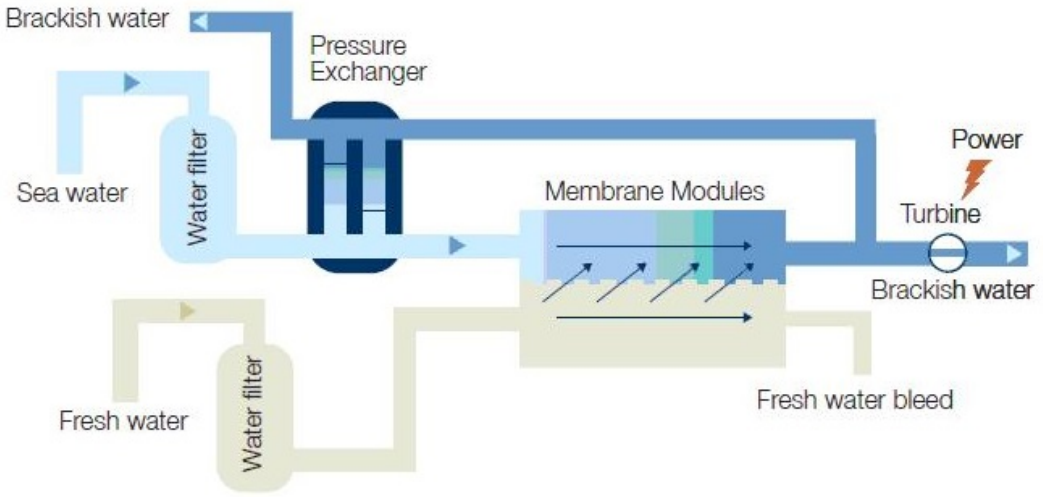

Figure 1: Schematic representation of a pressure retarded osmosis (PRO) power plant by Statkraft [1].

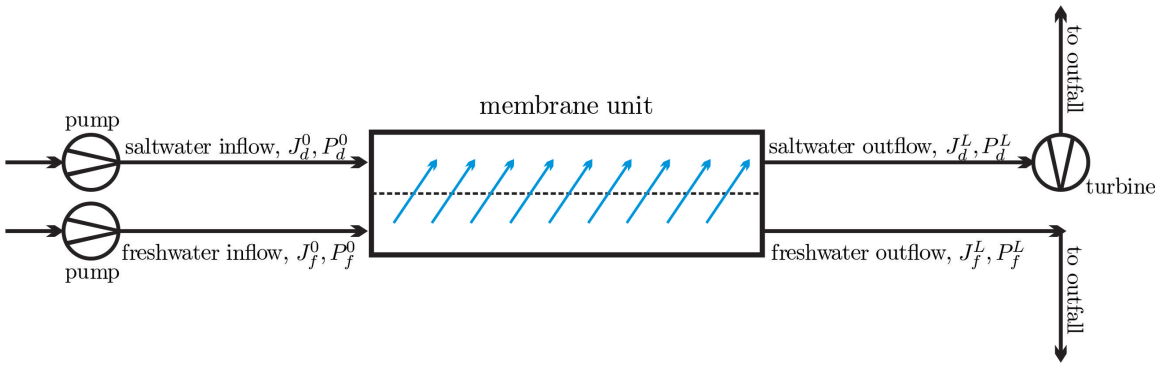

Figure 2: Schematic representation of a pressure-retarded osmosis (PRO) power plant with the pump-turbine setup.

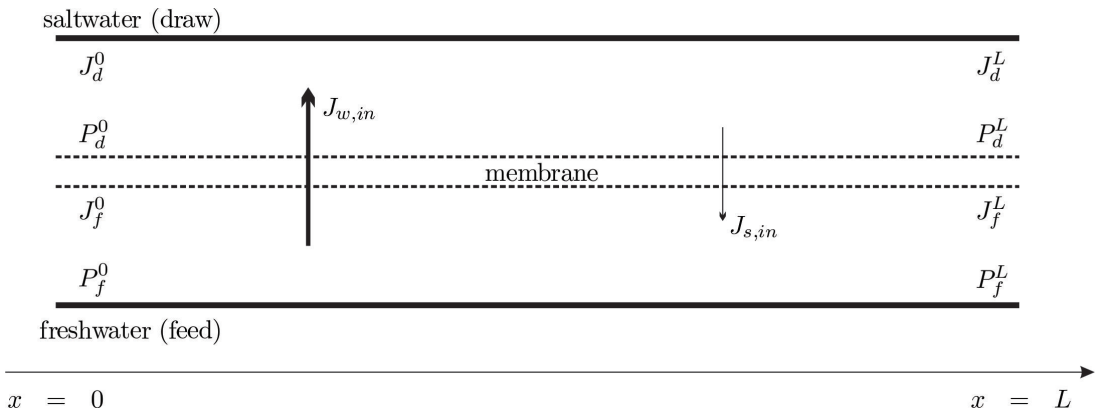

Figure 3: Cross-section through the membrane assembly along the flow. Saltwater at P_d^0 enters the membrane unit at $x = 0$ with initial draw flow J_d^0. Osmotic forces draw water from the feed to the draw side of the membrane ($J_{w,in}$) and salt in the opposite direction ($J_{s,in}$). Obstacles provide mixing of permeate water and saltwater. Increased draw flow exits the membrane unit at J_d^L with reduced pressure P_d^L.

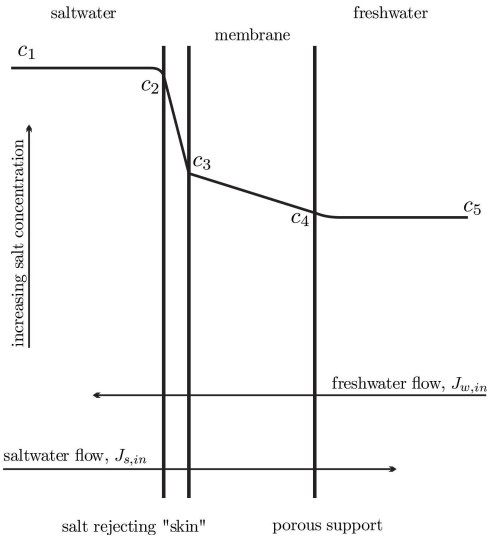

Figure 4: Cross-section of the membrane unit across the flow; c_i are the salt concentration values: c_1 – draw side of the membrane, c_2 – membrane surface on the saltwater part, c_3 – inside membrane porous support, c_4 – membrane surface on the freshwater part, c_5 – feed side of the membrane [11]. We denote by π_i the related osmotic pressures.

Quantity	Reference value	Typical reference value
length x	$x_r = L$	$1\ m$
pressure P	$P_r = P_E = P_f^L$	$10^5\ kgm^{-1}s^{-2}$
density ρ	$\rho_r = \rho_w$	$10^3\ kgm^{-3}$
flux J	$J_r = \sqrt{H^3 x_r P_r \rho_r}$	$10^{-2}\ kgs^{-1}$

Table 1: Scaling table with typical reference values

Water permeability	A	2.5×10^{-9}	s/m
Structure parameter	S	1×10^{-4}	m
Height	H	1×10^{-3}	m
ICP mass transfer coefficient	K	10^2	$m^2 s/kg$
Temperature	T	297	K
Length	L	2	m
Width	Z	1	m

Table 2: Input data for the membrane sample [11]

Temperature	T_0	297	K
Water mass density	ρ_W	1000	kg/m^3
Salt mass density	ρ_S	2165	kg/m^3
Water molecular weight	M_W	18	$kg/kmol$
Salt molecular weight	M_S	58.44	$kg/kmol$
Water gas constant	R_w	462	$J/kmolK$
Saltwater viscosity	η	1.3×10^{-3}	$kg/(ms)$
Incoming salinity	$C_d^0 = \hat{J}_{sd}^0/\hat{J}_{wd}^0$	$35/983$	
Incoming salt water salt mass fraction	$\hat{J}_{sd}^0/\hat{J}_d^0$	$35/1018$	
Incoming salt water water mass fraction	$\hat{J}_{wd}^0/\hat{J}_d^0$	$983/1018$	
Pump and turbine efficiency	$\epsilon_P = \epsilon_T$	0.95	
Salt Rejection	R	94%	

Table 3: Input data for fixed quantities

Salt flux in fresh water	$J_{sf}(x)\|_{x=0} = J_{sf}^0$	0	kg/s
Water flux in fresh water	$J_{wf}(x)\|_{x=0} = J_{wf}^0 = J_f^0$	0.01353	kg/s
Salt flux in saltwater	$J_{sd}(x)\|_{x=0} = J_{sd}^0$	$\frac{35}{1018}$ 0.01353	kg/s
Water flux in saltwater	$J_{wd}(x)\|_{x=0} = J_w^0$	$\frac{983}{1018}$ 0.01353	kg/s
Saltwater pressure	$P_s(x)\|_{x=0} = P_s^0$	$1.151 \cdot 10^6$	Pa
Fresh water pressure	$P_f(x)\|_{x=0} = P_f^0$	$1.1 \cdot 10^5$	Pa

Table 4: Initial conditions

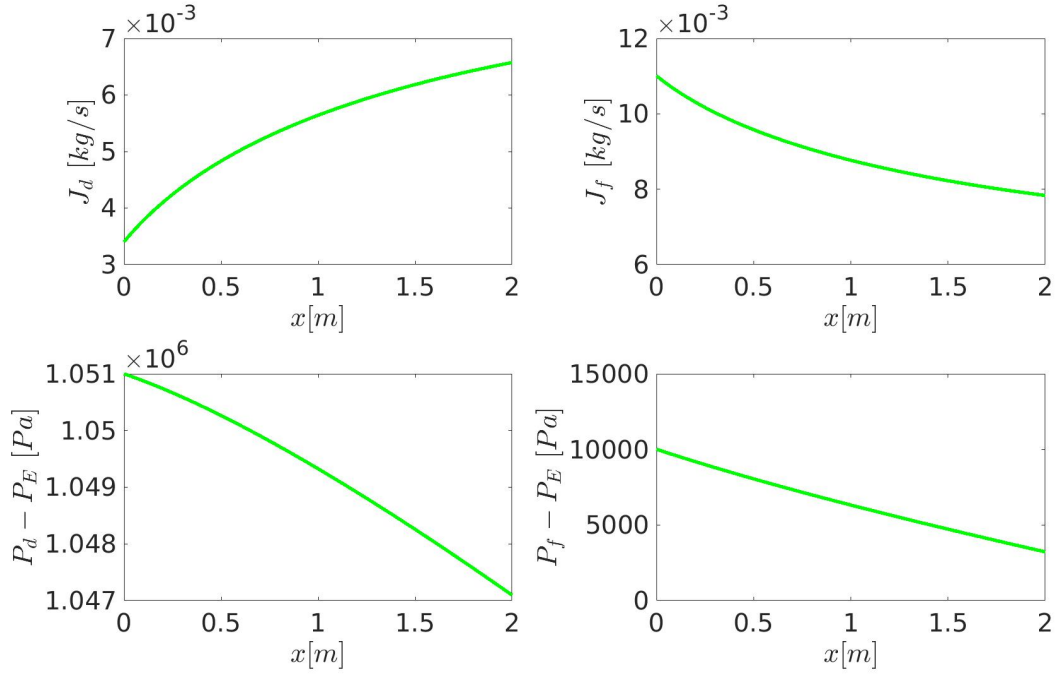

Figure 5: Sea water flux J_d and pressure P_d, and fresh water flux J_f and pressure P_f along x.

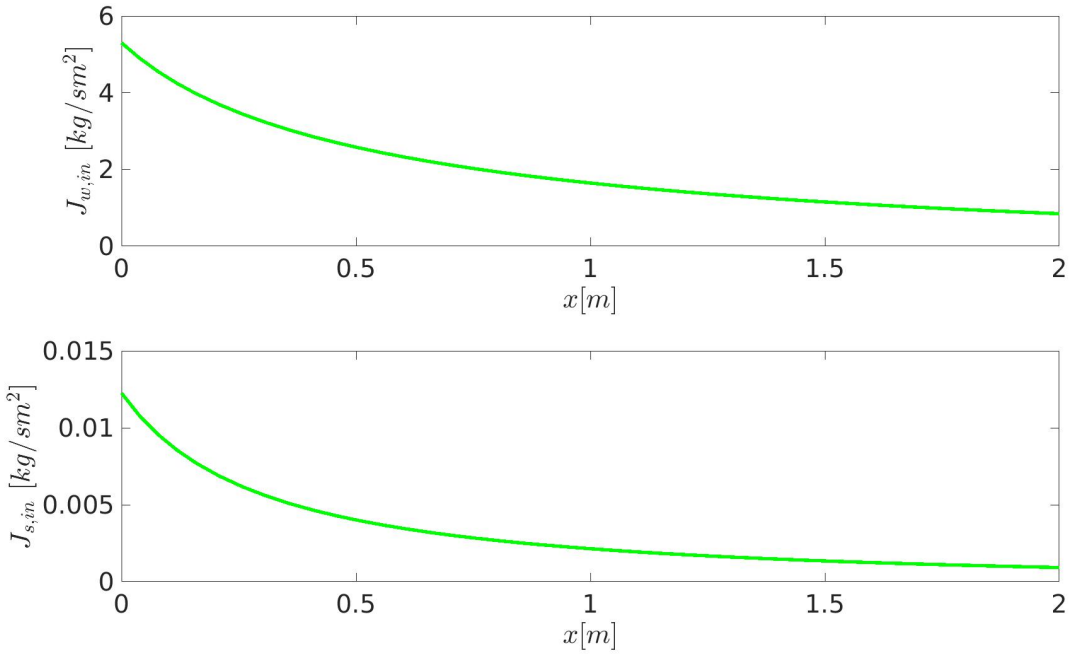

Figure 6: Water flux $J_{w,in}$ and salt flux $J_{s,in}$, across the membrane, along x.

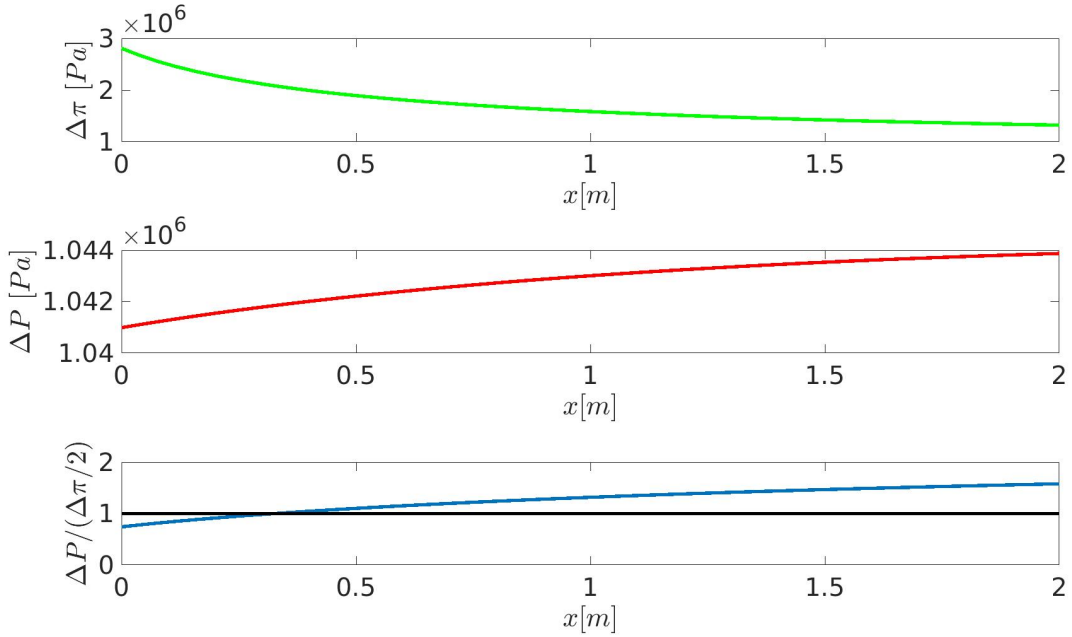

Figure 7: Osmotic pressure $\Delta\pi$, hydraulic pressure difference ΔP, and their ratio, along x.

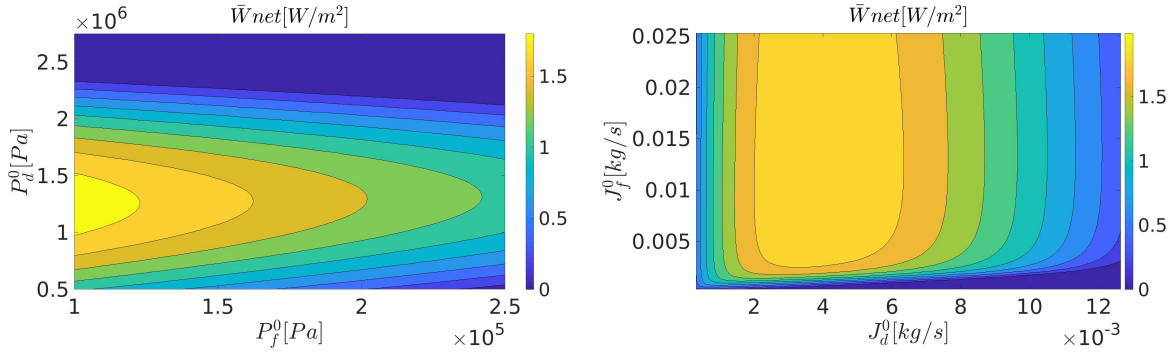

(a) **(b)**

Figure 8:
(a) Power per membrane area as function of hydraulic pressures P_d^0 and P_f^0, maximal value at $P_f^0 = 10^5$ Pa and $P_d^0 = 1.25 \cdot 10^6$ Pa.
(b) Power per membrane area as function of inlet draw and feed flows J_d^0 and J_f^0, maximal value at $J_f^0 = 0.0117$ kg/s and $J_d^0 = 0.0038$ kg/s.

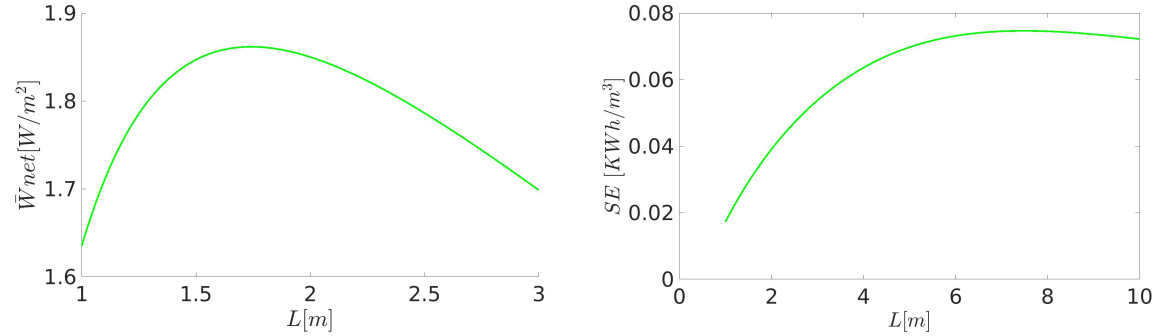

(a) **(b)**

Figure 9:
(a) Power per membrane area as function of membrane length L, maximal value at $L = 1.7474$ m.
(b) Specific energy as function of membrane length

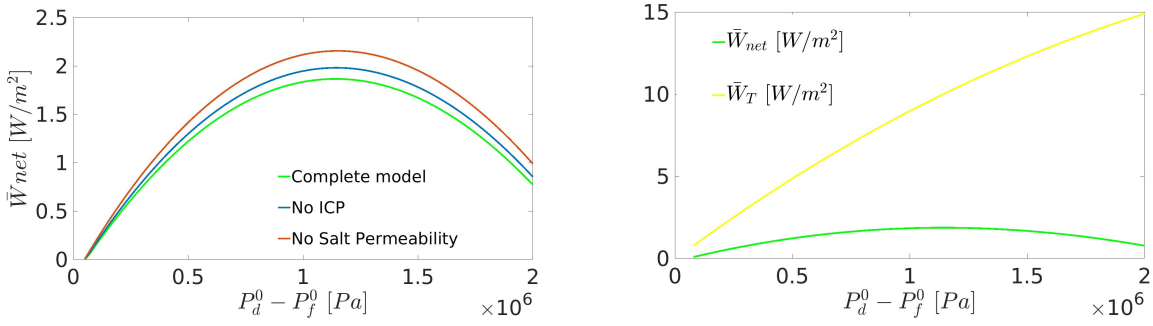

(a) **(b)**

Figure 10:
(a) Comparing the complete model ($\max(\bar{W}_{net}) = 1.86\ Watt/m^2$), with a model that does not take into account the effects of internal concentration polarization ($\max(\bar{W}_{net}) = 1.98\ Watt/m^2$) and a model for a membrane completely impermeable to salt ($\max(\bar{W}_{net}) = 2.15\ Watt/m^2$).
(b) Comparing the net power generated for membrane area $\bar{W}_{net}$ to $\bar{W}_T$, the power per membrane area generated in the turbine, in the complete model.

Data in $x = 0$		
Saltwater pressure (pump)	$P_d(x)\|_{x=0} = P_d^0$	$1.151 \cdot 10^6 Pa$
Fresh water pressure (pump)	$P_f(x)\|_{x=0} = P_f^0$	$1.1 \cdot 10^5 Pa$
Salt flux in fresh water	$J_{sf}(x)\|_{x=0} = J_{sf}^0$	0 kg/s
Fraction of salt in saltwater	$C_d(x)\|_{x=0} = C_d^0$	$35/983$
Data in $x = L$		
Saltwater pressure (turbine)	$P_d(x)\|_{x=L} = P_d^L$	$1.141 \cdot 10^6 Pa$
Fresh water pressure (-)	$P_f(x)\|_{x=L} = P_f^L = P_E$	$10^5 Pa$

Table 5: Boundary conditions

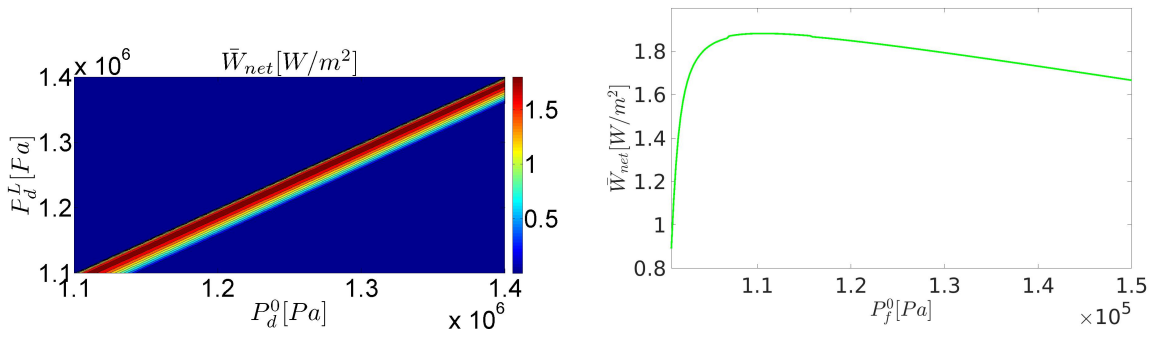

(a) **(b)**

Figure 11:
(a) Dependence on P_d^0 and P_d^L of net power per membrane unit area. Maximal net power at $P_d^0 = 1.247 \cdot 10^6$ and $P_d^L = 1.2349 \cdot 10^6$.
(b) Dependence on P_f^0. Maximal net power at $P_f^0 = 1.1061 \cdot 10^5$.

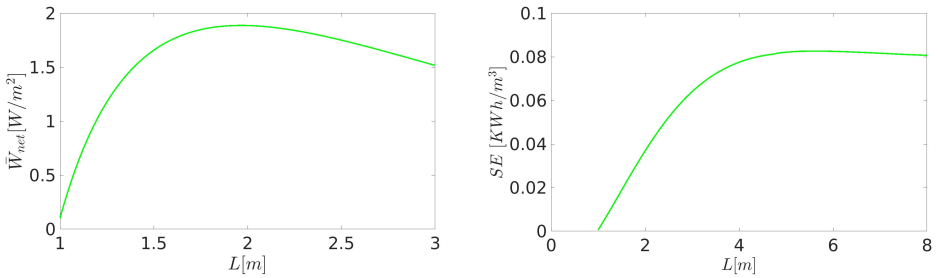

(a) **(b)**

Figure 12:
(a) Dependence of net power on membrane length. $Max(W_{net}) = 1.899\ W/m^2$, at $L = 1.9293\ m$.
(b) Dependence of specific energy on membrane length.

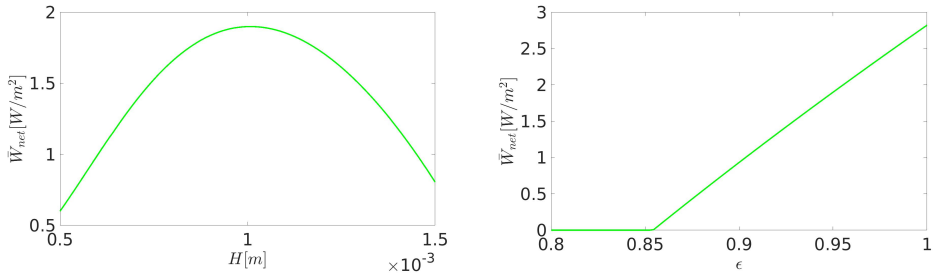

(a) **(b)**

Figure 13:
(a) Dependence of net power on channel hight. $Max(W_{net}) = 1.899\ W/m^2$, at $H = 0.001\ m$.
(b) Dependence on of net power on pump and turbine efficiency. Minimum efficiency required: $\epsilon_P = \epsilon_T > 0.852$.

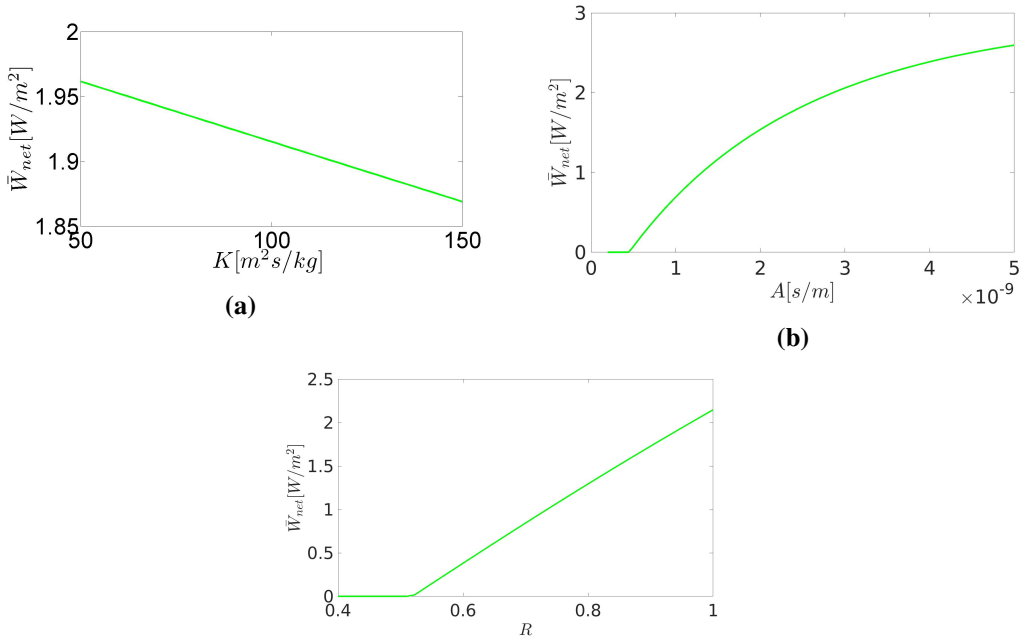

(a) **(b)**

(c)

Figure 14:
(a) Dependence on membrane ICP mass transfer coefficient K.
(b) Dependence on membrane water permeability A. Minimum required $A > 0.4424 \cdot 10^{-9}\ s/m$.
(c) Dependence on membrane salt rejection R. Minimum required: $R > 0.5102$.

Quantity	Symbol
Height of the membrane unit	H
Width of the membrane unit	Z
Length of the membrane unit	L
position along the membrane unit	x
Salt flux in fresh water/salt flux in fresh water per with	J_{sf}, $\hat{J}_{sf}$
Water flux in fresh water/water flux in fresh water per with	J_{wf}, $\hat{J}_{wf}$
Flux in fresh water/flux in fresh water per with	J_f, $\hat{J}_f$
Salt flux in salt water/salt flux in salt water per with	J_{sd}, $\hat{J}_{sd}$
Water flux in salt water/water flux in salt water per with	J_{wd}, $\hat{J}_{wd}$
Flux in salt water/flux in salt water per with	J_d, $\hat{J}_d$
Water flux through the membrane from fresh to salt water	$J_{w,in}$
Salt flux through the membrane fram salt to fresh water	$J_{s,in}$
Salt water mass density	ρ_d
Fresh water mass density	ρ_f
Water mass density	ρ_W
Salt mass density	ρ_S
Water molecular weight	M_W
Salt molecular weight	M_S
Water mole fraction	X_w
Salt water volume flow	$\dot{V}_d$
Fresh water volume flow	$\dot{V}_f$
Salt water pressure	P_s
Fresh water pressure	P_f
Pressure difference	ΔP
Salt water part osmotic pressure	π_s
Fresh water part osmotic pressure	π_f
Osmotic pressure difference	$\Delta\pi$
Pump power salt water part	W_P^d
Pump power fresh water part	W_P^f
Turbine power	W_T
Net power	W_{net}
Salinity in the salt water part	C_d
Salt concentration difference	Δc
Reynolds number	Re_H
Friction coefficient	f_{mix}
Temperature	T_0
Water gas constant	R_w
Saltwater viscosity	η
Pump/turbine efficiencies	ϵ_P, ϵ_T
Salt Rejection	R
Water permeability	A
Salt permeability coefficient	B
Membrane structure parameter	S
Membrane tortuosity	τ
Membrane porosity	ϵ
Membrane thickness	t
ICP mass transfer coefficient	K

Table 6: List of symbols